MICROSTRUCTURAL EXAMINATION OF DEFORMATION IN IRRADIATED V-4CR-4TI COMPRESSION SPECIMENS – D. S. Gelles (Pacific Northwest National Laboratory)*

OBJECTIVE

The objective of this effort is employ compression testing on irradiated vanadium alloys in order to better understand deformation behavior in this class of materials.

SUMMARY

Microstructural examinations have been performed on a series of V-4Cr-4Ti cylindrical compression specimens in order to provide understanding of the observed deformation behavior. Compression testing showed that unirradiated specimens exhibited upper and lower yield points whereas following irradiation the yield stresses were much higher and no yield drop behavior was observed. Both conditions showed evidence of serrated yielding during testing at ~420°C. Microstructural examination of irradiated conditions revealed extensive precipitation making it difficult to observe dislocation structures. Interstitial Impurities were found to form a fine distribution of precipitates following irradiation at ~420°C. Interaction between these precipitates and glide dislocations is apparent.

PROGRESS AND STATUS

Introduction

Compression testing allows measurement of deformation of low ductility materials to considerably higher strains than are possible by tensile testing. It also allows for stress relaxation test to identify deformation processes. If specimens are cylindrical and of sizes comparable to TEM disks, a simple process for preparing specimens for microstructural examination is possible, using slicing and electropolishing procedures. In previous reports on V-4Cr-4Ti compression testing of unirradiated materials, [1,2] two heats (NIFS-1 and 832665) were examined at three test temperatures (RT,~250 ~and ~420°C), and showed upper and lower yield points with strains to ~20%. Results are shown in Figure 1a with the coed CA designation the US heat (832665). More recently, tests have been performed on specimens from the MFE-RB-17J irradiation experiment in HFIR,[3,4] with those results reprocduced in Figure 1b.[5] It can be noted that compared to the unirradiated specimens, irradiated specimens are considerably stronger and do not show upper and lower yield pints. Also, testing at ~432°C of both unirradiated and irradiated speciments shows evidence for serrated yielding (specimens CA06, CJ87, CJ89, CA02 and CA05). The purpose of this report is to describe microstructural development in several of these samples of interest.

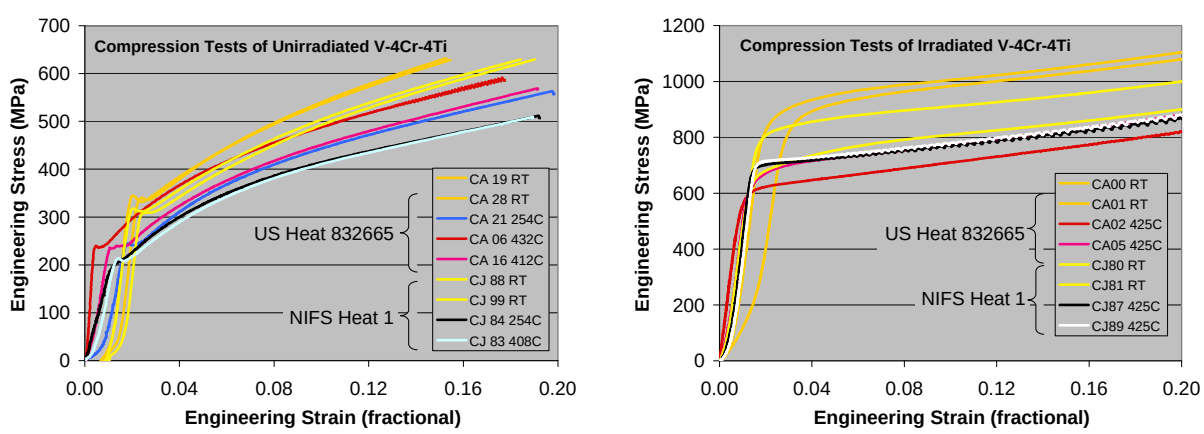

Figure 1. Compression test results of V-4Cr-4Ti for a) unirradiated and b) irradiated cylindrical samples.

---

* Pacific Northwest National Laboratory (PNNL) is operated for the U.S. Department of Energy by Battelle Memorial Institute under contract DE-AC06-76RLO-1830.

Experimental Procedure

Specimens selected for microstructural examination are listed in Table 1. These include specimens tested to ~20% as indicated in Figure 1 as well as one specimen, CA09, tested at RT to about 2% strain following irradiation and a second, CA10, untested following irradiation. Following compression testing, specimens tested to ~20% strain were barrel-shaped, indicating that strains were not completely uniaxial at the ends due to friction effects. Therefore, cylindrical specimens initially 3.0 mm in diameter were sectioned with a slow speed saw to provide only central slices ~.25 mm thick. Disks were then electrochemically thinned using standard procedures and examined in a JEM 2010F transmission electron microscope. This provided specimens for examination with the compression axis parallel to the electron beam when the sample was untitled. Images were collected digitally.

Table 1. Test conditions for specimens examined in this report.

Specimen ID	Test Temperature (°C)	~Strain (%)	Irradiation Dose (dpa)	Irradiation Temperature (°C)	Comments
CA19	RT	15			
CA16	412	18			
CJ88	RT	19			
CJ83	408	19			
CA10	Not tested	0	~2.5	425 [2]	
CA09	RT	2	~2.5	425	
CA00	RT	20	~2.5	425	

Results

Examinations are reported in the following order. The microstructure found in specimen CA09, a deformed sample of the US heat of V-4Cr-4Ti that was irradiated in the 17J test at 425°C to about 2.5 dpa and tested in compression at room temperature to approximately 2% strain, is compared with an undeformed duplicate, specimen CA10. Comparison is then made with specimen CA00, similar to CA09 but tested to ~20% strain. Finally, comparison is made with unirradiated conditions CA19 and CA16 tested at RT and 412°C, respectively and with CJ88 and CJ83, of the NIFS-1 heat, tested at RT and 408°C, respectively, all to ~20% strain.

The microstructure of as-irradiated V-4Cr-4Ti is complex, consisting of a high density of irradiation induced precipitates previously identified as [6-8] as “oxy-carbo-nitrides,” and dislocation loops and line segments, despite the low dose of ~2.5 dpa. Examples of the microstructure, comparing undeformed material with the ~2% deformation condition in CA09 are given in Figure 2, using imaging conditions best suited for observation of dislocations, $\bar{g}$=011. The area for CA10 is thicker than for CA09, but both contain small dark “black spot” features typical of precipitates, small dislocation loops on the order of 30 nm in diameter and longer dislocation line segments. Some differences can be identified by comparing these images. Many of the precipitates appear in stronger contrast following deformation, perhaps indicating that precipitates are decorated with circular dislocation rings retained following a dislocation bypass mechanism or deformed by a dislocation cutting through the particle to an internal fault. Also, regions can be indentified on the orderof 30 nm wide and 100 to 200 nm long following deformation that contain no precipitate or dislocation images, perhaps cleared of microsturctual features by deformation. However, both observations may be a result of differences in specimen thickness. Alternatively, it can be noted that the imaging conditions used should only allow observation of half the dislocations present, and these “cleared regions” may appear because not all Burgers vectors are imaged.

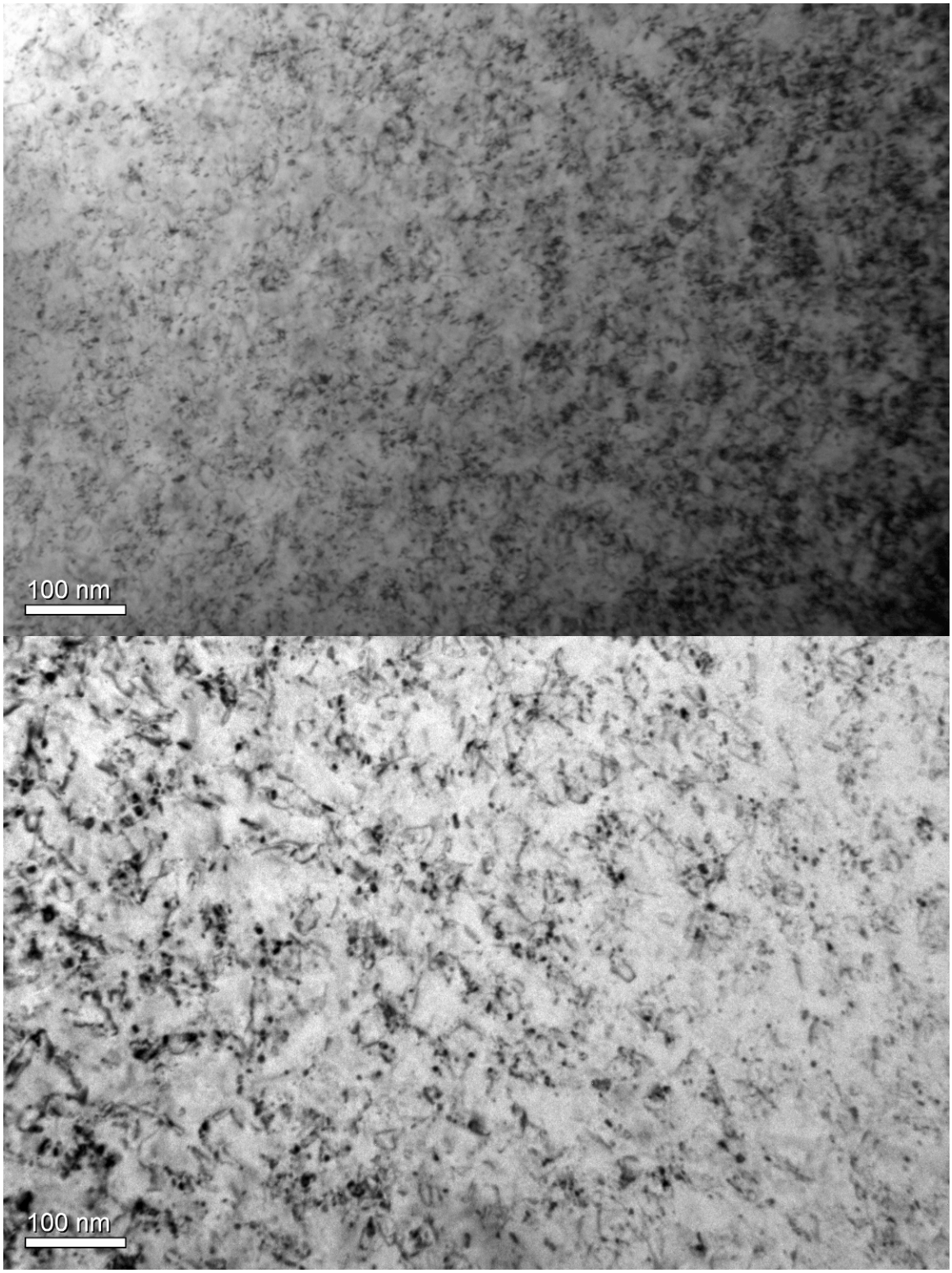

Figure 2. Comparison of microstructures in a) undeformed and b) deformed V-4Cr-4Ti, both irradiated at 425°C to ~2.5 dpa.

In order to ensure that deformation had indeed occurred following a strain of ~2%, attention was centered on a grain boundary area in each condition. Typically, a denuded zone develops free of irradiation-induced microstructure adjacent to grain boundaries during irradiation. Figure 3a shows such a boundary oriented from upper left to lower right in undefromed condition CA10. Denuded zones approximately 50 nm wide have developed on either side of the boundary. Figure 3b provides the comparison following deformation to ~2% strain in condition CA09, showing a typical grain boundary region oriented horizontally in dislocation contrast. Dislocations can be seen at several places, crossing the denuded zone adjacent to the boundary. Therefore, sufficient strain has been induced to cause dislocation slip bands to cross denuded zones in sample CA09 at a spacing of ~100 nm so that any typical region selected for examination can be expected to be deformed.

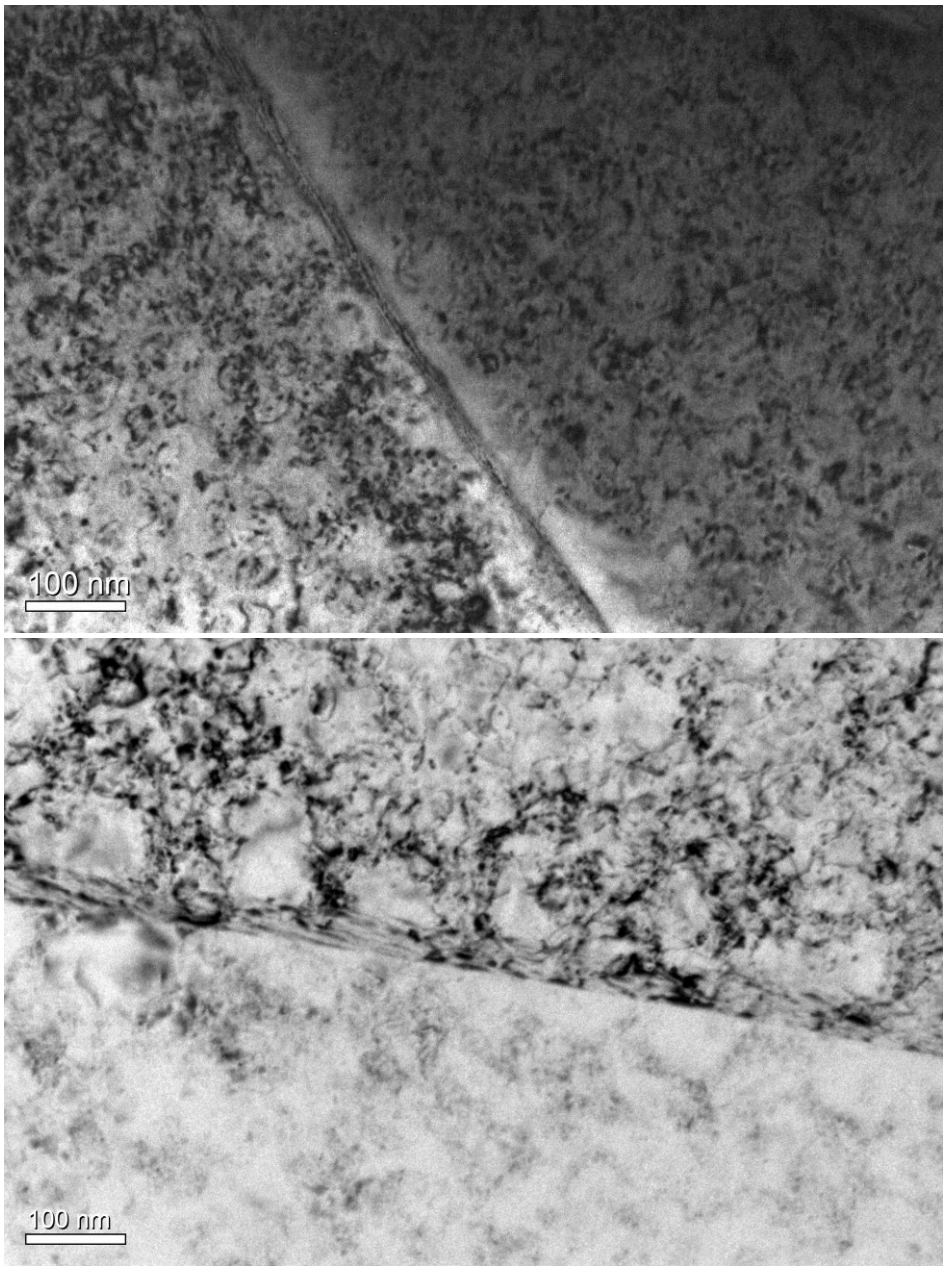

Figure 3. Dislocation structures near grain boundaries in conditions a) CA10, undeformed, and b) CA09, deformed to ~2%.

In an effort to better understand the microstructures due to deformation following irradiation, stereo pairs were taken of condition CA09 and are presented as anaglyphs, requiring the use of colored glasses for stereo observation. Figure 4 provides an anaglyph using $\bar{g}$=011 contrast showing the area in Figure 2b, and Figure 5 provides an anaglyph using weak beam $\bar{g}$=200 contrast, with the images inverted to better show the dislocation structures. Both images have been rotated to optimize stereo viewing, so that g is vertical. It can be noted that $\bar{g}$=200 imaging should show all dislocations present.

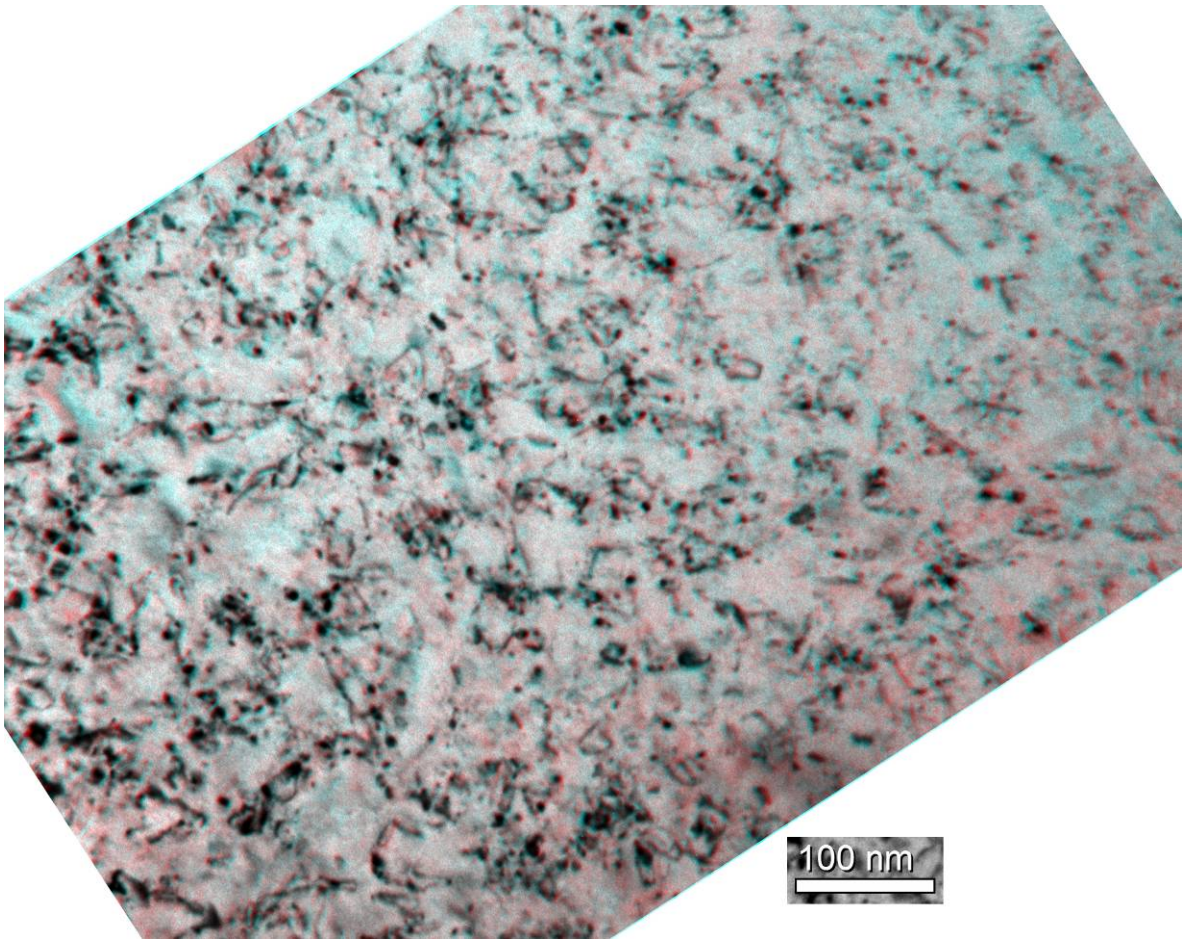

Figure 4. Anaglyph of dislocation structure in CA09 using $\bar{g}$=011 contrast for a foil near $(01\bar{1})$.

For those having difficulty seeing these images in stereo, a brief description will be provided based on standard viewing conditions with a red lens on the left. The stereo model for Figure 4 is only slightly inclined, with the thicker section on the right. Dislocation and precipitate features appear in vertical walls, often inclined to the vertical direction. A number of examples of (a/2)<111> loops on the order of 25 nm diameter or less can be identified with segments often obscured by overlying features, and both strongly contrasted and weakly contrasted “black spot damage” representing precipitates can be seen. The black spot features are describe as representing precipitates because two size distributions of loops are unlikely unless two different Burgers vectors are represented. This structure appears in patches, with intervening background of two shades, one grey and the other more white. It is possible to convince oneself that the white patches represent planar regions at a ~45° incline to the surface, and therefore they may define deformation bands. Also, examples can be found of straight dislocation segments, many of which are not associated with precipitate (black spot) decoration. The foil thickness is estimated, based on a convergent beam pattern for a nearby area is ~150 nm.

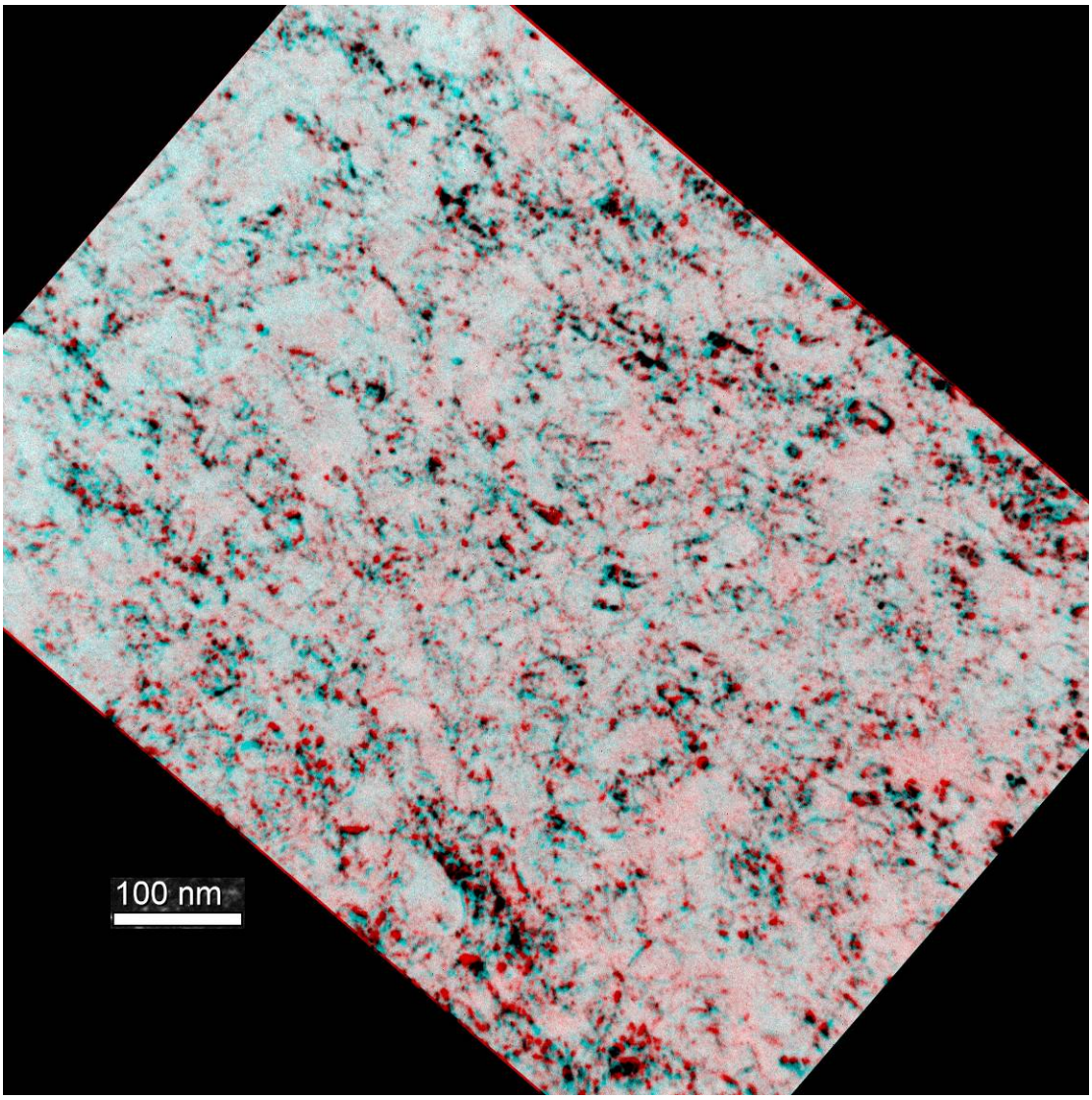

Figure 5. Anaglyph of dislocation structure in CA09 using $\bar{g}$=200 weak beam contrast with the image inverted for a foil near $(01\bar{1})$.

Figure 5 shows the same region using $\bar{g}$=200 contrast so that all (a/2) <111> dislocations can be seen. The stereo model is about three times deeper, and individual dislocation loops and line segments can be identified in weak contrast from top to bottom. Therefore the dislocation images are very narrow and weak, but in stereo, a dislocation network can be identified. Again, strongly and weakly contrasted "black spot damage" can be seen which tends to be clumped as a function of depth and structure is non-uniformly distributed, with some whiter background regions identifiable.

In order to better understand the consequences of much higher levels of deformation, Figure 6 has been prepared from specimen CA00 deformed ~20% following irradiation. The imaging conditions are the same as those in Figures 5 with the anaglyph image using inverted $\bar{g}$ =200 contrast with $\bar{g}$ vertical. The stereo model in this case is inclined with the lower left down and upper right up. Individual dislocations are difficult to identify, the structure appears to primarily consist of walls of clumped black spots or precipitates. Examples can be found in the central left area where black spots or precipitates are in linear arrays. Therefore, a much lower density of dislocations is apparent, probably because dislocations are masked by black spot features or at too high a density to be resolved. However, regions are again

apparent where little structure is visible, defining a cell wall structure with no internal structure that probably originated from the irradiated microstructure.

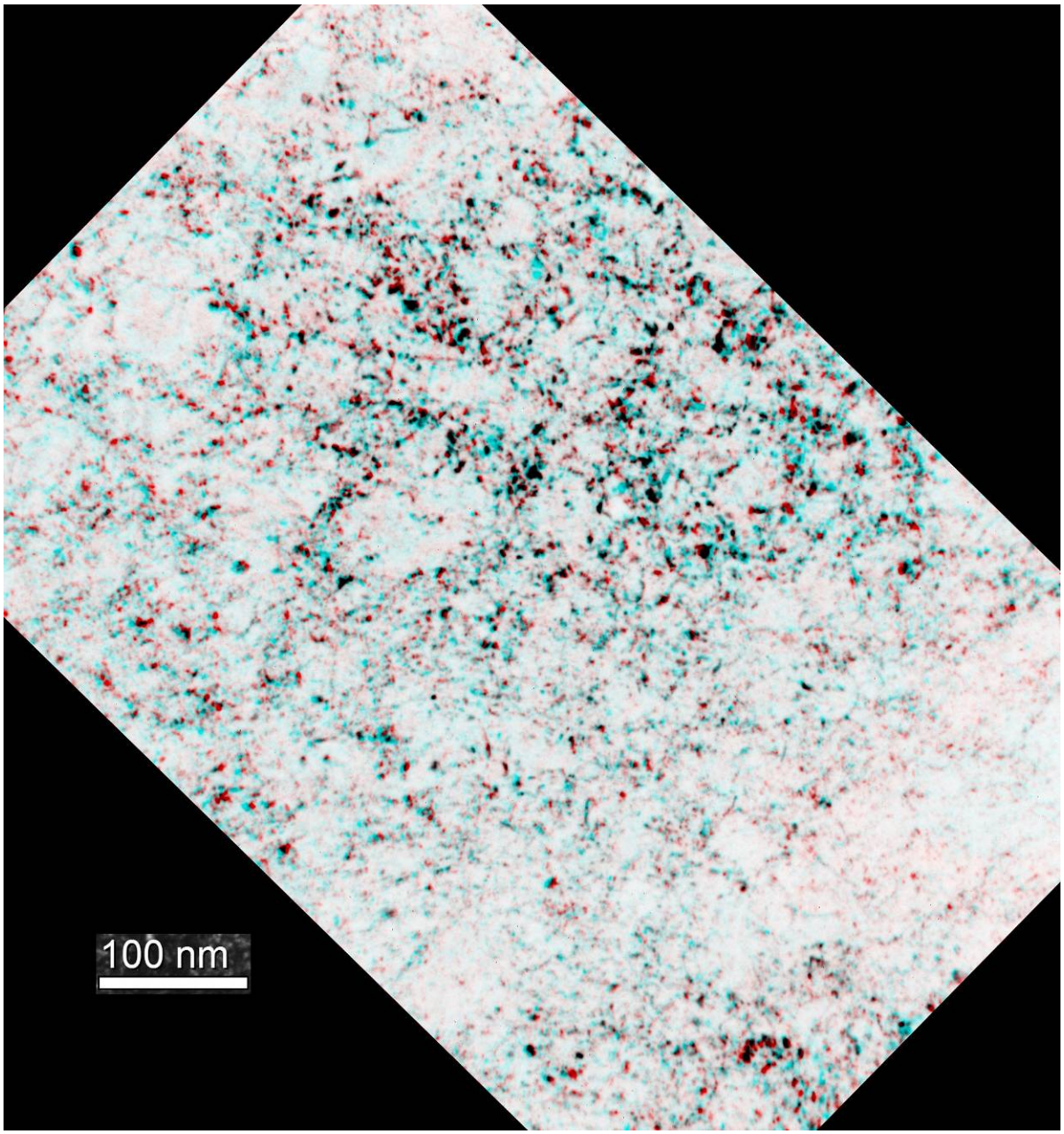

Figure 6. Anaglyph of dislocation structure in CA00 using $\bar{g}$=200 weak beam contrast with the image inverted for a foil near (001).

Figure 7 shows another example of the dislocation structure in CA00 in $\bar{g}$=011 contrast in order to provide comparison with Figure 2b (in part, for those unable to deal with the stereo images). The magnification is lower, so the dislocation density appears higher in CA00 than in CA09 and consisting of complex line segment networks. Of note is the fact that most precipitates appear in strong contrast whereas images of Ca09 and CA10 in Figures 2 and 3 show both precipitates appear in both strong and weak contrast. Appear at a higher density following deformation to 20% strain.

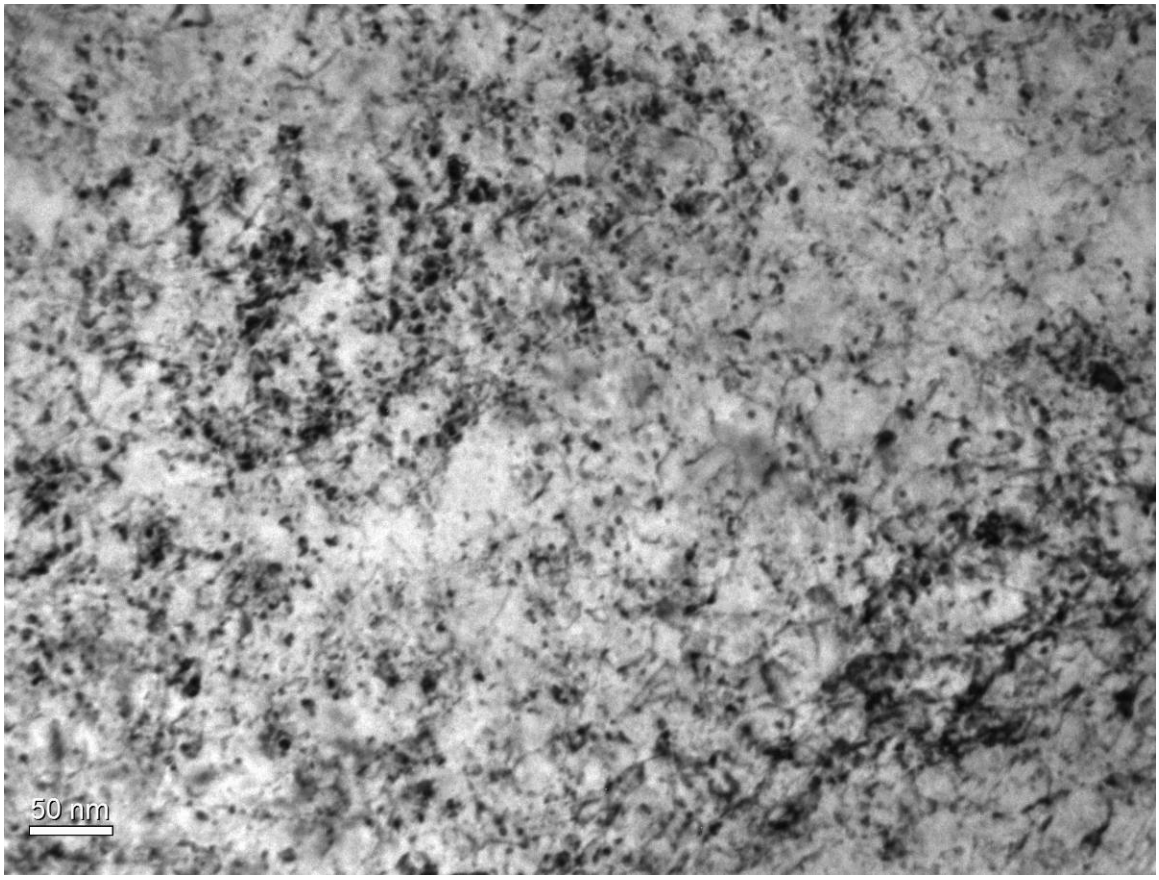

Figure 7. Dislocation and precipitate strictures in condition CA00 after irradiation at 425°C to ~2.5 dpa and ~20% strain.

Finally, examples are provided of microstructures in unirradiated conditions tested to ~20% strain. All images are for $\bar{g}$=110, with CA19, tested at RT in a), CA16, tested at 412°C in b), CJ88, tested at RT in c) and CJ83 tested at 408°C in d). Dislocations are clearly visible without precipitate particles do not appear to be present for the CA (or US heat) conditions, but surprisingly, a few precipitates can be seen for the CJ (or NIFS-1) heat conditions. The dislocation structure is less tangled following testing at the higher temperature, as expected. In comparison with the irradiated microstructures, the major difference is the precipitate (or black spot) density following irradiation.

Discussion

Microstructural studies have demonstrated that irradiation of V-4Cr-4Ti at temperatures around 425°C and below results in extensive precipitation of “oxy-carbo-nitrides” [6,7]. Higher irradiation temperatures do not show these features. Also, deformation tests on V-4Cr-4Ti following irradiation in this temperature range of 425°C, both in tension and compression, have repeatedly demonstrated significant hardening [5,9]. Furthermore, tensile and compression testing of both unirradiated and irradiated V-4Cr-4Ti demonstrate serrated yielding in the range 200 to 400°C [5,9,10]. It is apparent that the deformation properties of this material are dependent on the distribution and motion of interstitial oxygen, carbon and nitrogen present in the alloy and irradiation encourages precipitation.

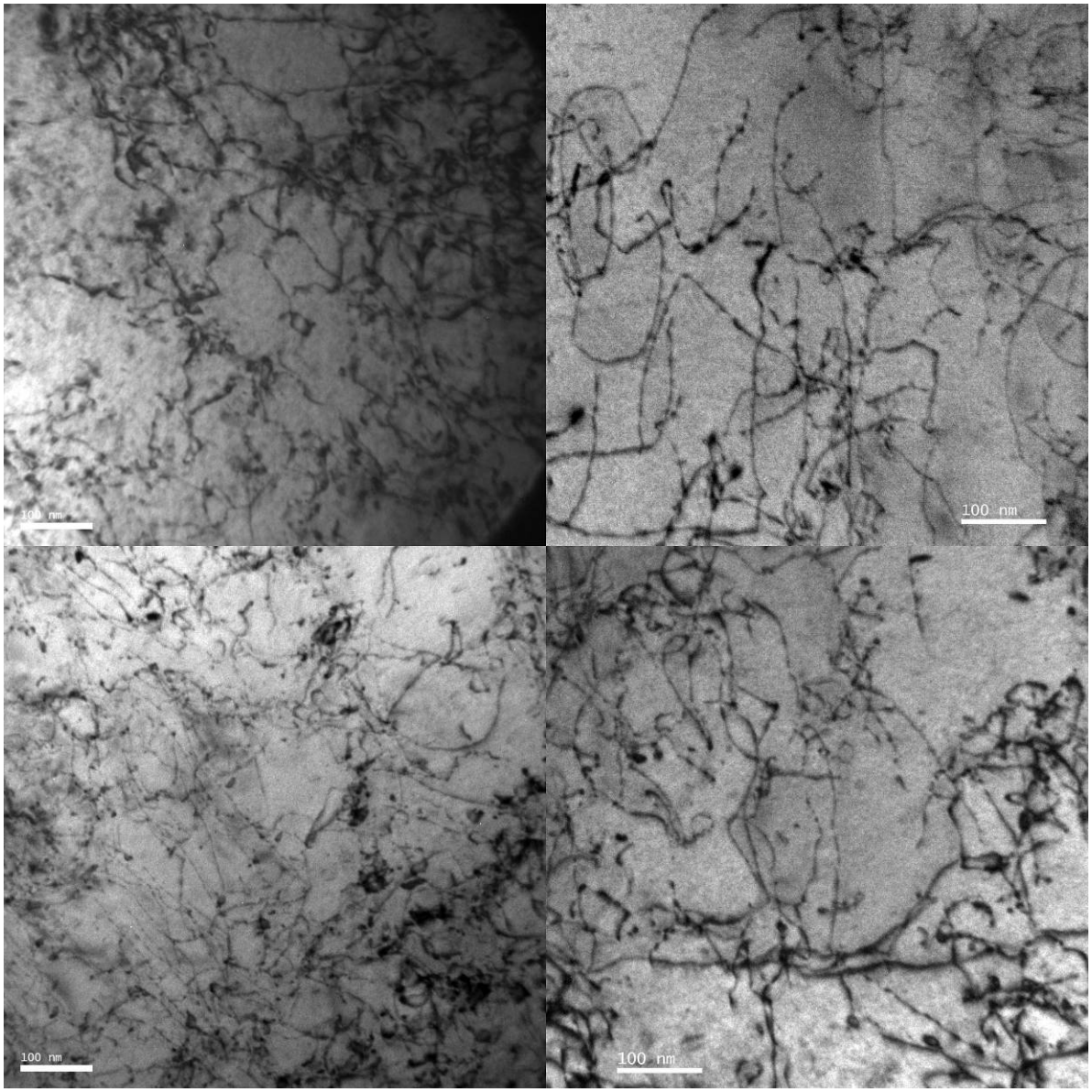

Figure 8, Microstructures in unirradiated conditions at ~20% strain with CA19, tested at RT in a), CA16 tested at 412° C in b), CJ88, tested at RT in c) and CJ83 tested at 408°C in d).

The present work confirms that irradiation induced dislocation structure is highly decorated with precipitation. In fact, several images taken in this study show precipitation localized into cell walls and in linear arrays indicating that precipitation is favored on growing dislocation loops, presumably by a solute segregation process. This can account for regions in the microstructure where precipitation is not prevalent because dislocations did not evolve there.

The dislocations formed in V-4Cr-4Ti are of the type (a/2)<111>, and if no obstacles exist and applied stresses are sufficiently high, they are free to glide on glide planes or cylinders that contain the Burger's vector. Irradiation at ~425°C to ~2.5 dpa raises yield strength by a factor of two. It is apparent from the microstructures presented here for specimens tested at RT following irradiation, and predicted by earlier work, that the irradiation induced precipitates are responsible for the hardening observed. We have not observed extensive planar slip band deformation except in denuded grain boundary regions, (and do not expect to see it in a microstructure containing high precipitate densities).

However, it is noted that serrated yielding was observed for several irradiated specimens tested in compression at ~425-500°C,[5,9]. As irradiation induced precipitation is understood to remove the oxy-carbo-nitrides that cause serrated yielding, this result is surprising. Either significant solute concentrations remain in solution following irradiation, or solute is released during deformation. Evidence for the latter can be noted based on the observation that the extent of serrated yielding increases with strain (or time at temperature.) [5,9] Further studies should be worthwhile, including stress relaxation tests, which may provide a measure of the solute in the vicinity of dislocations, as a function of hold time so as to differentiate between deformation-induced and thermal dissolution.

Conclusions

The mechanism controlling deformation at room temperature in V-4Cr-4Ti was shown to be extensive precipitation, in some measure due to solute segregation. No evidence for extensive planar slip band formation was found.

Future Work

The effort will be continued as opportunities become available.

References

[1] M. B. Toloczko and R. J. Kurtz, in DOE/ER-0313/36 (2004) 131.
[2] M. M. Fryd, M. B. Toloczko and R. J. Kurtz, in DOE/ER-0313/39 (2006) 11.
[3] D. K. Felde, A. L. Qualls, K. R. Thoms, D. W. Heatherly, R. G. Sitterson and R. L Wallace, in DOE/ER-0313/36 (2004) 120.
[4] D. K. Felde, and R. L Wallace, in DOE/ER-0313/38 (2005) 159.
[5] M. B. Toloczko, to be reported.
[6] D. S. Gelles, P. M. Rice, S. J. Zinkle and H. M. Chung, "Microstructural Examination of Irradiated V-(4-5%)Cr-(4-6%)Ti," *J. Nucl. Mater.* V 258-263 (1998) 1380.
[7] D. S. Gelles, "Microstructural Examination of V-(3-6%)Cr-(3-5%)Ti Irradiated in the ATR-A1 Experiment," *J. Nucl. Mater.* V 283-287 (2000) 344.
[8] H. M. Chung, M. C. Billone, and D. L. Smith, in DOE/ER-0313/22 (1998) 22.
[9] A. F, Rowcliffe, S. J. Zinkle and D. T. Hoelzer, J. Nucl. Mater., 283-287 (2000) 508.
[10] D. T. Hoelzer and A. F, Rowcliffe, J. Nucl. Mater., 307-311 (2002) 596.